

# ASSESSMENT OF THE SPATIAL CORRELATION OF WATER VAPOUR, LIQUID WATER AND RAIN AMOUNTS IN EUROPE, NORTH AMERICA AND JAPAN USING ECMWF RE-ANALYSIS DATA

Antonio Martellucci<sup>(1)</sup>, Lorenzo Luini<sup>(2)</sup>, Andrea Testoni<sup>(2)</sup>,  
Aldo Paraboni<sup>(2)</sup>, Carlo Riva<sup>(2)</sup>

<sup>(1)</sup> *European Space Agency, ESTEC, TEC-EEP, Keplerlaan 1, PB 299, NL-2200 AG Noordwijk, The Netherlands,  
E-mail: [antonio.martellucci@esa.int](mailto:antonio.martellucci@esa.int)*

<sup>(2)</sup> *Dipartimento di Elettronica e Informazione, Politecnico di Milano, Piazza L. da Vinci 32, 20133 Milano (Italy),  
Email: [luini@elet.polimi.it](mailto:luini@elet.polimi.it)*

## INTRODUCTION

The aim of this study is to investigate the spatial correlation of water vapour, liquid water and rain amounts over Europe, North America and Japan. The study has been performed exploiting ERA-15 (concerning rain) and ERA-40 (concerning water vapour and liquid water) re-analysis data from ECMWF, considering at least 15 years, to assure the proper statistical stability to the results. In particular the Statistical Dependence Index  $\chi$  [1] (SDI) has been calculated and its variation with distance has been considered.

## THE STATISTICAL DEPENDENCE INDEX

The Statistical Dependence Index  $\chi$  is a useful tool to study spatial correlation. Defining  $P_a$ ,  $P_b$  as the cumulative distribution function (CDF) of, for example, the water vapour amount accumulated over 6 hours, for a given pixel  $a$ ,  $b$  and  $P_{ab}$  as the joint probability relative to both pixels  $a$  and  $b$ , the Statistical Dependence Index  $\chi$  is given by:

$$\chi_{ab} = \frac{P_a}{(P_a \cdot P_b)} \quad (1)$$

where:  $P_a = \Pr(W_a > W_t)$ ,  $P_b = \Pr(W_b > W_t)$  and  $P_{ab} = \Pr(W_a > W_t, W_b > W_t)$ , being  $W_t$  the water vapour amount exceeded. The value  $\chi = 1$  represents statistical independence.

## SPATIAL CORRELATION

For each ERA pixel over one region, the CDF of the total column of water vapour, liquid water and rain, with a 6-hour integration interval (standard ERA time resolution), has been calculated (Figure 1.1). This operation has been performed for the three following regions:

- Europe:  $35^\circ \text{ N} < \text{latitude} < 75^\circ \text{ N}$  and  $12.5^\circ \text{ W} < \text{longitude} < 42.5^\circ \text{ E}$ ;
- North America:  $30^\circ \text{ N} < \text{latitude} < 70^\circ \text{ N}$  and  $130^\circ \text{ W} < \text{longitude} < 60^\circ \text{ W}$ ;
- Japan:  $24^\circ \text{ N} < \text{latitude} < 52.5^\circ \text{ N}$  and  $120^\circ \text{ E} < \text{longitude} < 156^\circ \text{ E}$ .

In order to evaluate the SDI index and therefore to investigate the spatial variation of a meteorological variable, a proper exceedance threshold has to be chosen such that it is common to all the CDFs and, moreover, it allows to consider only values of probability higher than  $10^{-3}$ , thus guaranteeing statistical stability to the results (considering 15 years of data, 6-hour sampled,  $10^{-3}$  probability means almost 22 samples in this exercise). As it can be seen in Figure 1.1, both 2 mm/6h and 5 mm/6h, for example, are acceptable thresholds to study the spatial correlation of rain over the Japanese area. Considering now the threshold of 2 mm/h, the SDI can be calculated between every pixel and all the others belonging to the selected region. Figure 1.2 shows the SDI variation with distance: each point refers to one value of  $\chi$  (in log scale) associated to the great circle distance (the shortest surface distance) between the two considered pixels. The red line in the graph, i.e.  $\log(\chi) = 0$ , or  $\chi = 1$  indicates total independence. In Figure 1.2, two different populations can be immediately identified: some points reach total independence, some others instead are still over the red line, even at a distance of 4000 km. More precisely, we can identify three main areas:

- between 0 and 1000 km, where there is a strong decay of  $\chi$  (the first independent points can be found at 500 km)
- between 1000 and 2000 km, where a slow decrease of  $\chi$  can be observed
- from 2000 km on, where  $\chi$  is almost constant, showing both dependent and independent behavior of the samples.

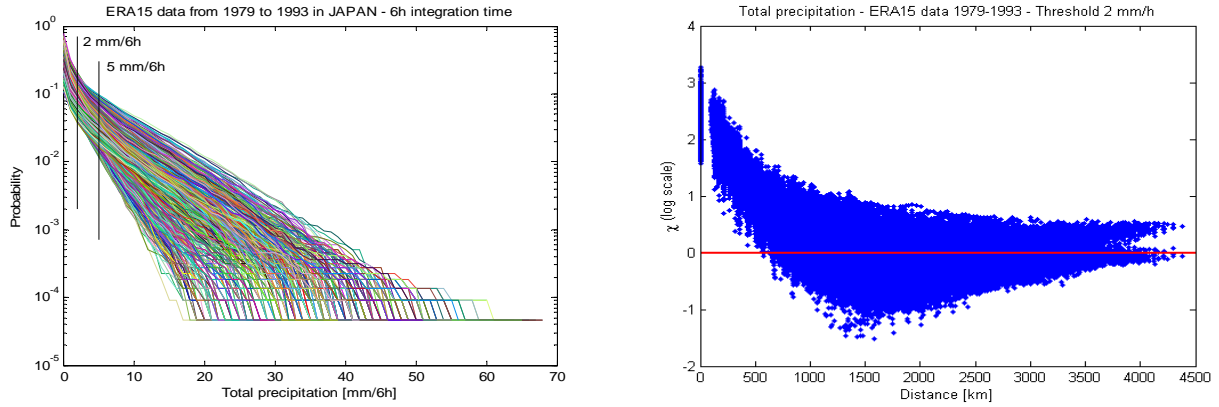


Figure 1: Japan - CDFs for all the pixels (each line refers to one pixel) (1) and variation of  $\chi$  with distance, total precipitation with threshold of 2 mm/6h (2)

Figure 2.1 and Figure 2.2 show the trend of  $\chi$  as a function of the distance for specific latitude and longitude belts. Each line represents the average over all longitudes or latitudes pixels at the same distance, contained in, respectively, a latitude or a longitude line. In the figures,  $\chi$  seems to depend more on latitude than on longitude: more precisely, it is easy to underline that statistical independence is reached within a shorter distance at Southern than at Northern latitudes. Concerning longitude belts, a peak of dependence is visible around 500 km. Finally,  $\chi$  asymptotic value is greater for longitude belts than for latitude ones: this fact may explain the two populations of points which are visible in Figure 1.2.

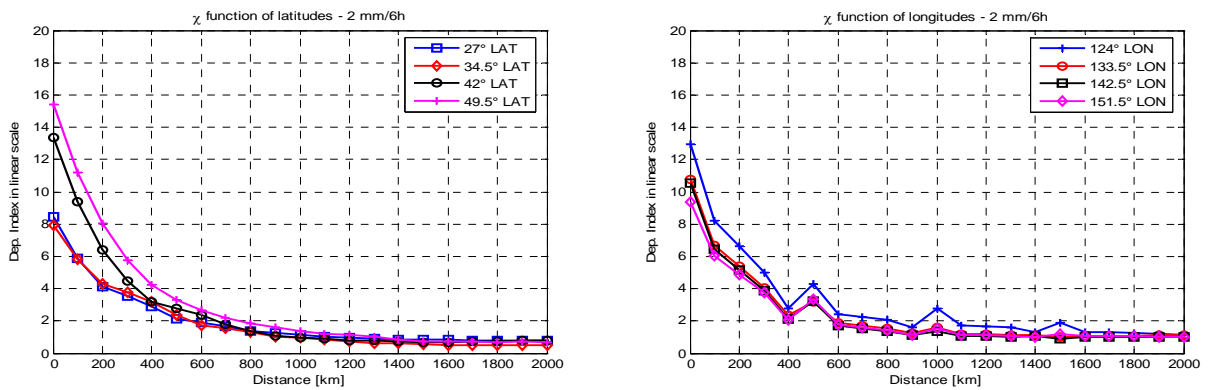
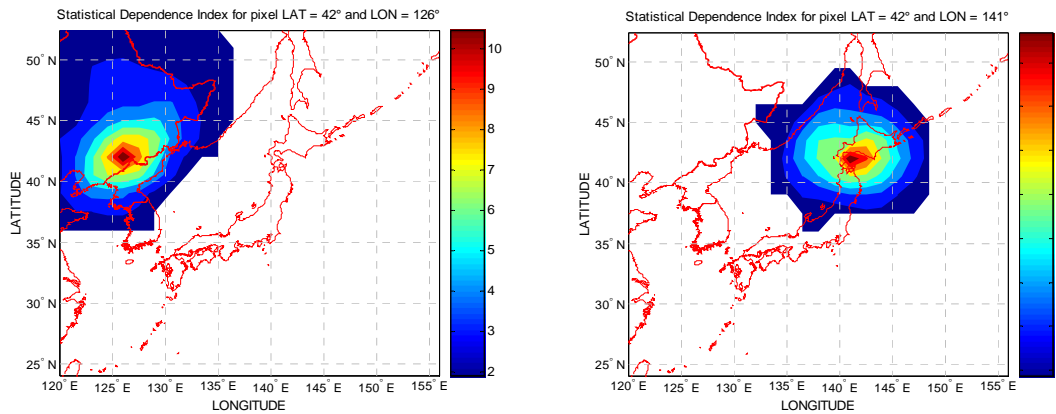


Figure 2: Japan - dependence index, averaged over all longitudes pixels at the same distance, contained in a latitude line (1) and vice versa (2). Total precipitation with threshold of 2 mm/6h

To better understand the spatial variation of  $\chi$ , the following maps in Figure 3 show some examples of the spatial correlation over Japan.



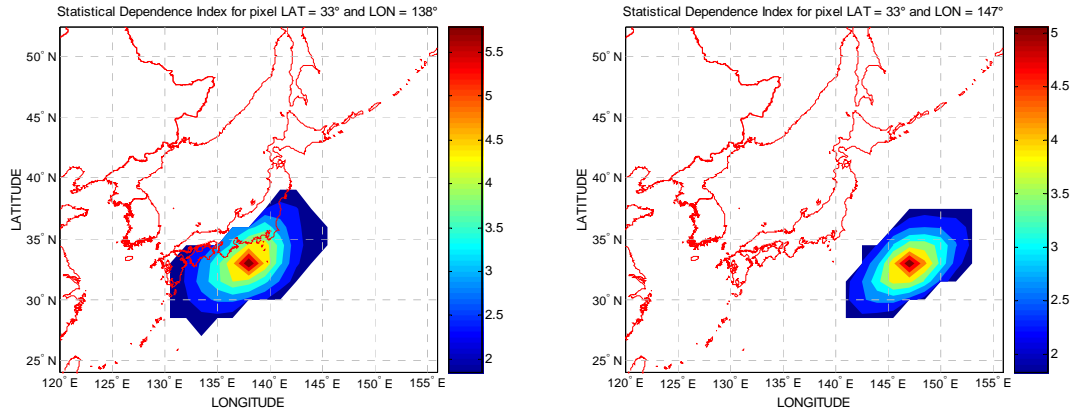
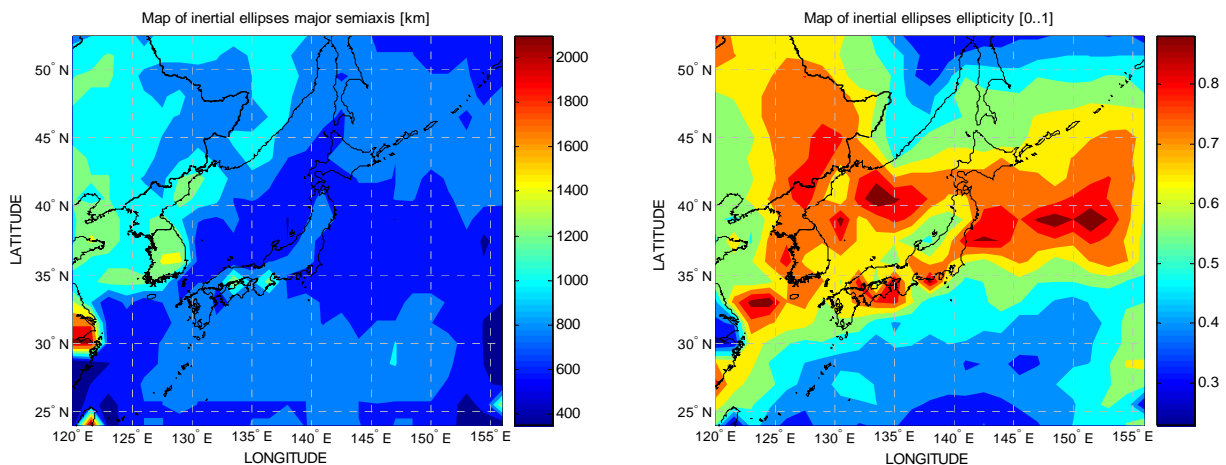


Figure 3: spatial variation of  $\chi$  between one pixel and all the others of the map. Total precipitation with threshold of 2 mm/6h (from left to right, from top to bottom, subfigures are numbered from 1 to 4)

In the maps,  $\chi$  has been set thresholded to 1.8. In Figure 3, it is possible to underline some general characteristics (this kind of investigation has been performed for many pixels): a) when considering pixels over the ocean, the correlation is limited to a narrow area (like in Figure 3.4); b) when considering pixels over the land, the correlation is wider and it seems to be affected by topography: this effect can be mainly seen in Figure 3.1, but also in Figure 3.2. In particular, in Figure 3.3, the distribution of  $\chi$  tends to follow the western coastal line of Japan; c) finally, as already pointed out in Figure 2.1, it is easy to notice that the total rain spatial correlation, concerning this region, is wider at Northern latitudes than at Southern ones.

To have a more complete view of the spatial distribution of  $\chi$  over Japan, the correlation spots (like the ones in Figure 3), have been modelled by means of ellipses of inertia. In particular, for each pixel over the region, the major semiaxis length  $a$ , the ellipticity  $e$  and the orientation angle  $\theta$  (with respect to west-east direction) of the equivalent inertial ellipse have been computed. For each pixel, the centre of the ellipse has been made coincident with the pixel itself; the correlation spots, considered to obtain the ellipses, are made up only of  $\chi$  values greater than 1.8 (the same threshold used in Figure 3). Figure 4 summarizes the characteristics of the equivalent inertial ellipses parameters, calculated over all the scene.

Figure 4.1 gives a confirmation of the fact that the correlation is wider on the land than on the ocean, since all higher values of the major semiaxis are concentrated on the continental part of the map, i.e. Korea and Russia. Concerning the orientation angle, although it is not possible to identify a main inclination value for the whole region in Figure 4.2, it is easy to notice how the rain fronts over the ocean show a similar orientation (for example consider the belt of latitudes between 25° N and 30° N), while there is a strong and rapid variation of the inclination in proximity of coastal lines: it is another sign of the topography influence on total rain spatial correlation.



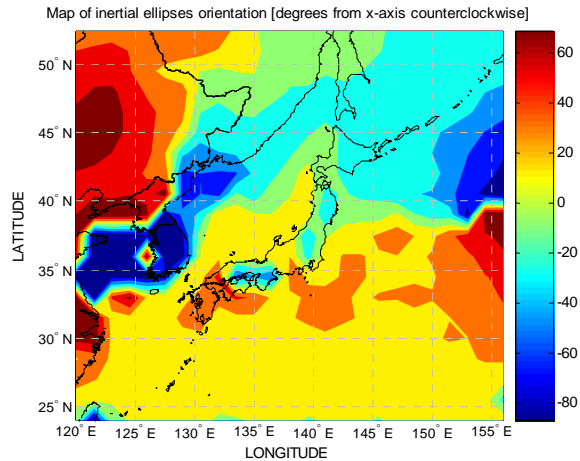


Figure 4. Distribution of the values of the inertial ellipses parameters

## CONCLUSIONS

Concerning the spatial correlation of total rain over Japan, analyzing  $\chi$  behavior with distance, it is possible to notice that independence is reached from 500 km on, although, even at long distances (i.e. 4000 km), some  $\chi$  values still indicate the lack of total independences. The trend of  $\chi$  with distance seems to depend more on latitudes than on longitudes, and, more precisely, the spatial correlation is wider at Northern latitude belts. Finally, as expected,  $\chi$  distribution is affected by topography: correlation spots are wider and more irregular on the land than on the ocean and the orientation angle of the equivalent inertial ellipses shows strong and rapid variations, mainly in proximity of coastal lines. The same kind of investigation has been performed concerning rain amounts over Europe and North America (exploiting ERA-15 data) and concerning water vapour and liquid water contents over Europe, North America and Japan. General conclusions can be drawn:

- rain amounts: in the first 1000 km, a steep decrease in the SDI can be noticed, afterwards a smaller decrease is found until 3000 km, finally total statistical independence is reached, sometimes with a slight return of correlation in the middle. The SDI is strongly affected by topography (it seems to be wider over the land than over the ocean and to be affected by coastal lines) and orography (mountains usually limit its extent). Results on stratiform rain are very similar to those of total rain shown above, while, concerning convective rain, it has been concluded that the geographical resolution of the available dataset ( $1.5^\circ \times 1.5^\circ$ ) is too poor to analyze this kind of precipitation, which are characterized by quite a limited spatial extent
- water vapour: real statistical independence is hardly reached, which points out the small variability of water vapour in space and time. A wider correlation over the land with respect to over the ocean has been observed (it may depend on heating from the soil, man made pollution, ...). Strong influence coming from orography has been noticed (a clear example is given by the Rocky Mountains in the USA)
- liquid water: the SDI trend with distance has been found to be very similar to the one of rain, although correlation seems to be wider over the ocean with respect to over the land; again the SDI spots are strongly affected by topography and orography.

The same kind of investigation is easily achievable, starting from other ERA meteorological variables, through the software that has been implemented (MATLAB) in accomplishing this study.

## ACKNOWLEDGEMENTS

This work was partially funded by ESA/ESTEC Contract No. 17877/04/NL/JA (“Reconfigurable Ka band antenna front end for active rain fade compensation”) and the European Union Cost Action 280 (“Propagation Impairment Mitigation for Millimetre Wave Radio Systems”) and technical and scientific support by ONERA.

## REFERENCES

- [1] F. Barbaliscia, G. Ravaioli and A. Paraboni, “Characteristic of the spatial statistical dependence of rainfall rate over large areas”, *IEEE Transactions on antennas and propagation*, vol. 40 (1), January 1992.